



Dynamics of DNA: Experimental controversies and theoretical insights

Michael Hinczewski^{a,b,*}, Roland R. Netz^a

^a Physics Department, Technical University of Munich, 85748 Garching, Germany

^b Institute for Physical Science and Technology, University of Maryland, College Park, MD 20742, USA

ARTICLE INFO

Article history:

Received 4 February 2010

Available online 12 February 2010

Keywords:

DNA

ABSTRACT

Recent experimental advances using fluorescence correlation spectroscopy (FCS) have given unprecedented information about the small-scale kinetics of large biopolymers in solution. However some of the first studies in this direction yielded conflicting results for the mean squared displacement of the tagged end-point of a DNA chain, deviating from traditional theories of polymer dynamics. Spurred by this controversy, we have developed a hydrodynamic mean-field theory for single semiflexible polymers which points to a resolution of the differing experimental observations. The theory precisely captures, without fitting parameters, one set of recent FCS results, reproducing the experimental dynamics over five decades in time and three decades of chain lengths. The success of the theory makes it an excellent candidate for a variety of biophysical contexts where the internal fluctuations of semiflexible polymers play a role.

© 2010 Elsevier B.V. All rights reserved.

1. Introduction

Developments in single-molecule experimental techniques in recent years have opened up the possibility of studying the detailed dynamics of biomolecules in solution, and testing our fundamental theoretical understanding of this behavior. For the case of double-stranded DNA, fluorescence correlation spectroscopy (FCS) can reveal DNA kinetics at the level of a single monomer [1–3], but the experimental picture has been clouded by conflicting results. Two studies, first by Shusterman et al. [2] and subsequently by Petrov et al. [3], have used FCS to extract the mean squared displacement (MSD) of a fluorescent tag attached to the end of double-stranded DNA molecules of various contour lengths $L = 0.1$ – 20 kbp (≈ 30 – 7000 nm). The DNA solutions are sufficiently dilute that in principle this technique can investigate the intersegmental fluctuations of single chains, directly probing the relation between the underlying elastic structure of the DNA and the resulting dynamics.

Representative results from both studies for comparable L are shown in Fig. 1(a)–(c), with the end-point MSD, $\Delta_{\text{end}}(t)$, plotted as a function of time t on a log–log scale. Since the MSD is typically analyzed in terms of power-law scaling, the bottom panels show the corresponding local slopes $\alpha_{\text{end}}(t) = d \log \Delta_{\text{end}}(t) / d \log t$. The most surprising aspect of these results are indications of an “intermediate Rouse regime” in the Shusterman et al. data: for sufficiently long chains, the MSD follows an approximate scaling $\Delta_{\text{end}}(t) \propto t^{1/2}$ ($\alpha_{\text{end}}(t) \approx 1/2$) for a wide time range corresponding to polymer motion at length scales smaller than the coil size but larger than the persistence length l_p (≈ 150 bp or 50 nm for DNA). This regime is consistent with the free-draining Rouse model of flexible polymers, which neglects long-range hydrodynamic coupling between different points on the chain contour. However for dilute solutions these hydrodynamic interactions are expected to be significant, and lead to non-draining behavior that is qualitatively described by the Zimm theory, which predicts a scaling exponent $\alpha_{\text{end}}(t) = 2/3$ [4]. Indeed, the Petrov et al. data, while agreeing with the earlier results at large times, shows a markedly different behavior in the intermediate and short time regimes: their MSD is 2–3 times smaller, and scales with an exponent closer to the Zimm prediction.

* Corresponding author at: Physics Department, Technical University of Munich, 85748 Garching, Germany.

E-mail address: mhinczewski@ph.tum.de (M. Hinczewski).

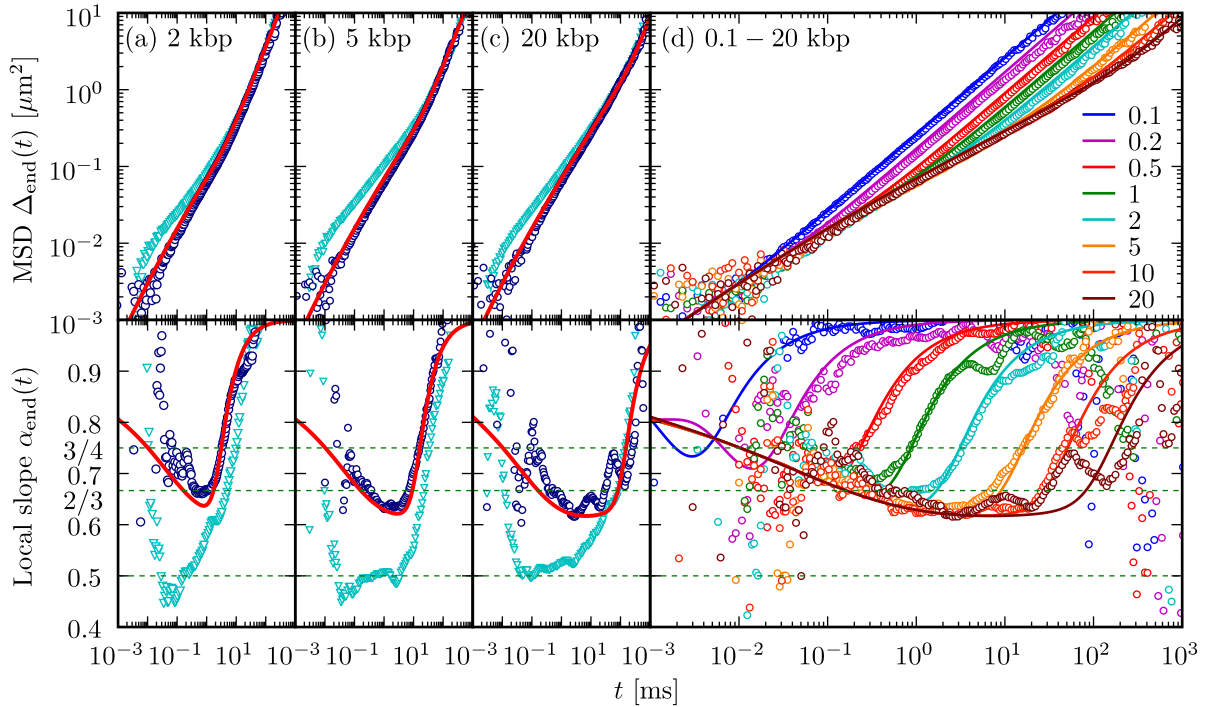


Fig. 1. (Color online) Top panels: $\Delta_{\text{end}}(t)$, the MSD of a tagged end-point in a double-stranded DNA chain of length (a) $L \approx 2$ kbp, (b) $L \approx 5$ kbp, (c) $L \approx 20$ kbp, and (d) various $L \approx 0.1$ –20 kbp. In (a)–(c), two series of FCS experimental results are compared: Shusterman et al. [2] (triangles) and Petrov et al. [3] (circles). For (a)–(c) the exact values of L in the former experiment are 2400, 6700, and 23,100 bp, while in the latter they are 1965, 5058, and 19,941 bp. In (d) only the Petrov et al. results are shown. In (a)–(d) the solid curves are theoretical MFT predictions, without fitting parameters [5]. When used in the MFT the small differences in L in the experimental comparison do not lead to significant deviations on the scale of the figure. Bottom panels: the local slope $\alpha_{\text{end}}(t) = d \ln \Delta_{\text{end}}(t) / d \ln t$, calculated at each t by fitting straight lines to the log-log plots of the $\Delta_{\text{end}}(t)$ curves within a range time range t_i defined by $|\log_{10} t_i / t| < 0.15$.

While there is still no definitive experimental explanation for this discrepancy, we review here our recent theoretical efforts to try to shed some light on the controversy (for a more detailed treatment, see Refs. [5,6]). Constructing a quantitatively accurate dynamical theory for the end-point MSD of a semiflexible polymer like DNA is non-trivial: asymptotic scaling theories for flexible polymers like that of Rouse and Zimm cannot capture the complex crossovers that occur in the semiflexible case, which manifest themselves in the continuous variation of $\alpha_{\text{end}}(t)$ with t in the experimental data. The short time behavior (not clearly captured by the current experiments), consists of motion on length scales smaller than l_p , and should be dominated by bending stiffness (with an expected exponent $\alpha_{\text{end}}(t) = 3/4$ [7–9]). The precise nature of the intermediate time regime will crucially depend on the crossover occurring from this stiffness-dominated regime. The presence of long-range hydrodynamic interactions, which are often neglected in studying semiflexible polymer dynamics, further complicates the picture, inducing logarithmic (but experimentally observable) corrections in the scaling.

In our work, we have shown that one approach, based on a Gaussian mean-field theory (MFT) [10–13] for semiflexible polymer dynamics, can overcome these difficulties. Without any fitting parameters, its results for the end-point MSD are in excellent agreement with the Petrov et al. data over the entire range of measurements, covering three decades of chain length and five decades of time: it accurately models the complex cross-overs occurring between stiffness-dominated and flexible bending modes, along with larger-scale rotational and center-of-mass motion. The fact that our theory incorporates hydrodynamics, which may seem like merely a complicating factor, is actually a key element in its success. The long-range solvent-mediated coupling between different parts of the chain contour makes the mean-field description more realistic. The quantitative precision of the theory suggests that it can be fruitfully applied to a variety of problems involving semiflexible polymer dynamics.

2. Hydrodynamic mean-field theory for semiflexible polymers

We begin by briefly summarizing the MFT approach to semiflexible polymer dynamics [6,5]. Polymer stiffness is typically modeled by the worm-like chain (WLC) elastic energy [14], $U_{\text{WLC}} = \frac{1}{2} l_p k_B T \int ds (\partial_s \mathbf{u}(s))^2$, for a polymer contour $\mathbf{r}(s)$, $0 \leq s \leq L$, with persistence length l_p and tangent vector $\mathbf{u}(s) \equiv \partial_s \mathbf{r}(s)$. The restriction $|\mathbf{u}(s)| = 1$ at each s reflects the local inextensibility of the chain. Summing over all contours, the partition function $Z = \int \mathcal{D}\mathbf{u} \prod_s \delta(|\mathbf{u}(s)| - 1) \exp(-\beta U_{\text{WLC}})$, with the δ functions enforcing inextensibility and $\beta = 1/(k_B T)$. Since the $|\mathbf{u}(s)|$ constraint is nonlinear, calculating

dynamical quantities requires an approximation. The Gaussian mean-field model estimates Z through the stationary phase approach [11], $Z \approx \exp(-\beta \mathcal{F}_{\text{MF}}) = \int \mathcal{D}\mathbf{u} \exp(-\beta U_{\text{MF}})$, where the MFT Hamiltonian $U_{\text{MF}} = (\epsilon/2) \int ds (\partial_s \mathbf{u}(s))^2 + \nu \int ds \mathbf{u}^2(s) + \nu_0 (\mathbf{u}^2(0) + \mathbf{u}^2(L))$. Here we relax local inextensibility, and the parameters ν and ν_0 are determined through the stationary phase condition, $\partial_\nu \mathcal{F}_{\text{MF}} = \partial_{\nu_0} \mathcal{F}_{\text{MF}} = 0$. Thus ν and ν_0 act as Lagrange multipliers enforcing the global and end-point constraints $\int ds \langle \mathbf{u}^2(s) \rangle = L$, $\langle \mathbf{u}^2(0) \rangle = \langle \mathbf{u}^2(L) \rangle = 1$. By tuning the parameters, the Hamiltonian U_{MF} can be made to reproduce exactly the tangent–tangent correlation $\langle \mathbf{u}(s) \cdot \mathbf{u}(s') \rangle = \exp(-|s - s'|/l_p)$ of a WLC with persistence length l_p , as well as related thermodynamic averages.

Starting from this Gaussian approximation, the dynamics of the system are derived through a Zimm-like hydrodynamic pre-averaging approach [6,12]. The chain contour obeys the Langevin equation, $\partial_t \mathbf{r}(s, t) = -\int ds' \mu_{\text{avg}}(s - s') \delta U_{\text{MF}} / \delta \mathbf{r}(s', t) + \boldsymbol{\xi}(s, t)$, where $\boldsymbol{\xi}(s, t)$ are Gaussian stochastic velocities, and $\langle \xi_i(s, t) \xi_j(s', t') \rangle = 2k_B T \delta_{ij} \delta(t - t') \mu_{\text{avg}}(s - s')$ from the fluctuation–dissipation theorem. Here $\mu_{\text{avg}}(s - s')$ is the pre-averaged mobility tensor, obtained from the continuum Rotne–Prager tensor $\overleftrightarrow{\boldsymbol{\mu}}(s, s'; \mathbf{x})$ [12,15] describing long-range hydrodynamic coupling between two points s, s' on the contour at spatial separation \mathbf{x} . If a polymer configuration with points s and s' separated by \mathbf{x} has an equilibrium probability $G(s, s'; \mathbf{x})$, then the pre-averaged mobility is: $\int d^3 \mathbf{x} \overleftrightarrow{\boldsymbol{\mu}}(s, s'; \mathbf{x}) G(s, s'; \mathbf{x}) = \mu_{\text{avg}}(s - s') \overleftrightarrow{\mathbf{1}}$. To gauge the importance of hydrodynamic effects, we will also compare the free-draining case where long-range coupling is absent and the mobility $\mu_{\text{avg}}^{\text{fd}}(s - s') = 2a\mu_0 \delta(s - s')$. Here a is a microscopic length scale corresponding to the monomer radius, η is the viscosity of water, and $\mu_0 = 1/6\pi\eta a$ is the Stokes mobility of a sphere of radius a . The Langevin equation can be solved through normal mode decomposition, yielding a set of coupled stochastic partial differential equations for the normal mode amplitudes. These in turn are diagonalized, resulting in a set of decoupled equations which can be used to calculate any dynamical quantity of interest.

3. Results and discussion

Our analysis focuses on the end-point MSD, $\Delta_{\text{end}}(t) \equiv \langle (\mathbf{r}(L, t) - \mathbf{r}(L, 0))^2 \rangle$, measured by the FCS experiments. Superimposed as solid curves in Fig. 1(a)–(c) are the MFT predictions for $\Delta_{\text{end}}(t)$ and the associated $\alpha_{\text{end}}(t)$, calculated without any fitting parameters. The constants in the theory are taken from the experimental conditions and the literature: $T = 298$ K, $\eta = 0.891$ mPa s, $a = 1$ nm, a rise per bp of 0.34 nm, $l_p = 50$ nm. The agreement between the MFT and the Petrov et al. results is remarkable. While panels (a)–(c) show only the contour lengths where the Shusterman *et al.* data is available for comparison, a wider range of L was investigated in the later study, which is shown in full in Fig. 1(d). The MFT works well for every case: the average discrepancy in the time range $t = 10^{-1}$ – 10^2 ms, where there is the least scatter in the Petrov et al. FCS data, varies between 6%–25% for the different L . To obtain this close agreement without fitting parameters, the full set of equations for the MFT normal mode amplitudes must be diagonalized and solved, including the off-diagonal coupling between normal modes due to hydrodynamics. The discrepancies between the MFT and the Shusterman et al. data suggest that one may need to re-examine the experimental setup or analysis in Ref. [2].

As can be clearly seen in Fig. 1(d), with increasing L a scaling regime gradually emerges at intermediate times with $\alpha_{\text{end}} \approx 0.62$, slightly below the Zimm value of $2/3$. This sub-Zimm scaling and pronounced variation in $\alpha_{\text{end}}(t)$ with t , consequences of slow cross-over effects, are precisely captured by the MFT. At times beyond the largest relaxation time of the chain, $\alpha_{\text{end}}(t)$ approaches 1, and we cross-over to center-of-mass motion. As mentioned earlier, there should be another cross-over at short times, where the length scale of the fluctuations is comparable to the persistence length, $\Delta_{\text{end}}(t) \lesssim l_p^2 \approx 2.5 \times 10^{-3} \mu\text{m}^2$. Unfortunately in the time range where we should see this stiffness-dominated regime the FCS data is not well-resolved: there is too much scatter in the $\Delta_{\text{end}}(t)$ results when $t < 10^{-1}$ ms. Note that the MFT curves are still in excellent agreement even for the shortest chains studied, where $L \lesssim l_p$. For these short, stiff fragments we see essentially only the cross-over to center-of-mass diffusion, with $\alpha_{\text{end}}(t) \rightarrow 1$.

To understand the reasons behind the success of the MFT, we have also run detailed comparisons of the theory with Brownian dynamics (BD) simulations of worm-like chains [5], both with and without hydrodynamic interactions. Fig. 2 shows the comparison between simulation and MFT $\Delta_{\text{end}}(t)$ for a chain of length $L = 100a$ and varying l_p , going from the flexible case of $l_p/L = 0.1$, to the stiff one of $l_p/L = 2.0$. The regular theory/simulation results with hydrodynamic interactions (shown in blue) are contrasted to the free-draining case (shown in red). We see a marked difference in the accuracy of the theory between the two cases. In the time range $t = 10^1$ – $10^4 a^2/k_B T \mu_0$ the average error between the hydrodynamic MFT and simulation $\Delta_{\text{end}}(t)$ varies from 3%–15% for the different l_p , similar to the errors seen in the experimental comparison above. The free-draining MFT, on the other hand, noticeably overestimates the short-time $\Delta_{\text{end}}(t)$, and the average errors compared to the BD results are 4–8 times larger than in the hydrodynamic counterparts. This is also plainly seen in the local slopes plotted in the bottom panels of Fig. 2: the non-hydrodynamic MFT performs significantly worse. Though hydrodynamics introduces another level of complexity into our approach, the resulting MFT is quantitatively more successful than the simpler free-draining theory. This is consistent with a well-known aspect of mean-field theories: they work better in systems with long-range interactions. Due to hydrodynamics, every point on the chain is coupled to every other point, whereas for a free-draining polymer, the dynamics of a point on the chain are determined solely by the local WLC interactions. Thus a Gaussian mean-field description in the latter case is a worse approximation.

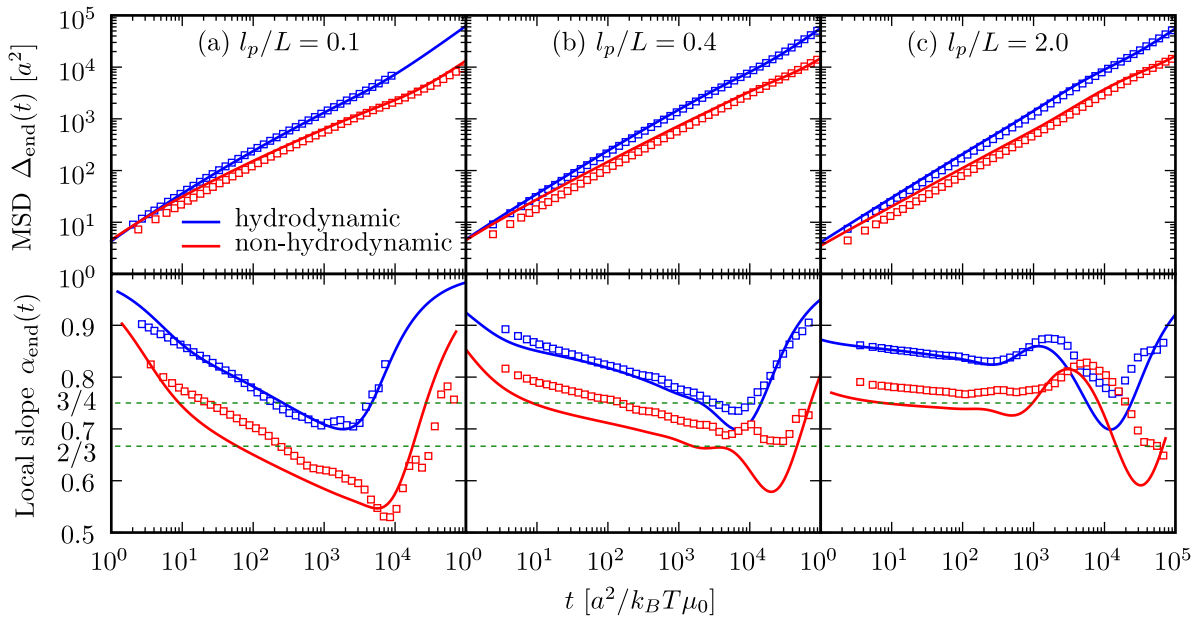


Fig. 2. (Color online) Top: $\Delta_{\text{end}}(t)$, the MSD of an end-point in a semiflexible polymer, for $L = 100a$ and three values of l_p/L ($a =$ monomer radius). Bottom: the local slope $\alpha_{\text{end}}(t) = d \ln \Delta_{\text{end}}/d \ln t$ of the log-log curves in the top panels. In all panels solid lines are MFT predictions, while squares are BD simulation data [5]. The upper curves (blue) include long-range hydrodynamic coupling, while the lower curves (red) are the free-draining results.

4. Outlook

The mean-field dynamical approach reviewed here gives a highly accurate description, without fitting parameters, of experimental FCS measurements on DNA. With this confirmation, we can confidently extend it to a variety of problems involving the internal fluctuations of semiflexible polymers. Two particular applications we have begun to explore are: (i) the competing effects of hydrodynamics and intersegmental diffusion of the DNA contour in determining the association rates of proteins binding to DNA [16]; (ii) the dynamics of DNA handles in optical tweezer force clamp experiments on single biomolecules. These handles attach the biomolecule to the polystyrene beads in the optical traps. In order to probe the biomolecule dynamics directly, the handle effects must be extracted out, and this requires a precise understanding of the DNA response under tension [17]. With these first steps, we hope that the hydrodynamic mean-field theory for semiflexible polymers will prove a versatile tool for the future.

Acknowledgements

Both authors express their deep gratitude to Nihat Berker on the occasion of his 60th birthday for his role as a wonderful teacher, relentless mentor and warm friend over the years. The research was financially supported by the Excellence Cluster “Nano-Initiative Munich”, and computing resources were provided by the Gilgamesh cluster of the Feza Gürsey Institute.

References

- [1] D. Lumma, et al., *Phys. Rev. Lett.* 90 (2003) 218301.
- [2] R. Shusterman, et al., *Phys. Rev. Lett.* 92 (2004) 048303.
- [3] E.P. Petrov, et al., *Phys. Rev. Lett.* 97 (2006) 258101.
- [4] M. Doi, S.F. Edwards, *The Theory of Polymer Dynamics*, Oxford University Press, 1988.
- [5] M. Hinczewski, R.R. Netz, *EPL (Europhys. Lett.)* 88 (2009) 18001.
- [6] M. Hinczewski, et al., *Macromolecules* 42 (2009) 860.
- [7] R. Granek, *J. Phys. II (France)* 7 (1997) 1761.
- [8] K. Kroy, E. Frey, *Phys. Rev. E* 55 (1997) 3092.
- [9] F. Gittes, F.C. MacKintosh, *Phys. Rev. E* 58 (1998) R1241.
- [10] R.G. Winkler, P. Reineker, L. Harnau, *J. Chem. Phys.* 101 (1994) 8119.
- [11] B.Y. Ha, D. Thirumalai, *J. Chem. Phys.* 103 (1995) 9408.
- [12] L. Harnau, R.G. Winkler, P. Reineker, *J. Chem. Phys.* 104 (1996) 6355.
- [13] R.G. Winkler, *J. Chem. Phys.* 127 (2007) 054904.
- [14] O. Kratky, G. Porod, *Rec. Trav. Chim. Pays-Bas* 68 (1949) 1106.
- [15] J. Rotne, S. Prager, *J. Chem. Phys.* 50 (1969) 4831.
- [16] Y. von Hansen, R.R. Netz, M. Hinczewski, [arXiv:0907.2573](https://arxiv.org/abs/0907.2573) (2009).
- [17] M. Hinczewski, R.R. Netz, [arXiv:0908.0376](https://arxiv.org/abs/0908.0376) (2009).